Iron-57 NMR Chemical Shifts and Mössbauer Quadrupole Splittings in Metalloporphyrins, Ferrocytochrome *c*, and Myoglobins: A Density Functional Theory Investigation†

Nathalie Godbout,‡ Robert Havlin,‡,¶ Renzo Salzmann,‡,# Peter G. Debrunner,⊥ and Eric Oldfield*,‡

Department of Chemistry, University of Illinois at Urbana−Champaign, 600 South Mathews Avenue, Urbana, Illinois 61801, and Department of Physics, University of Illinois at Urbana−Champaign, 1110 West Green Street, Urbana, Illinois 61801

Received: August 4, 1997; In Final Form: November 24, 1997

We have evaluated the ^{57}Fe nuclear magnetic resonance chemical shielding and Mössbauer electric field gradient tensors and their orientations for a cytochrome *c* model compound as well as for isopropyl isocyanide and carbon monoxy−myoglobin model systems and two simple metalloporphyrins containing bis(pyridine) and bis(trimethylphosphine) ligands, using Kohn−Sham density functional theory. For cytochrome *c* we used a model Fe(II) porphyrin structure together with a 1-methylimidazole base (to represent His-18) and a dimethyl sulfide molecule (to represent Met-80 in the structure of horse heart ferrocytochrome *c*), both located at the X-ray coordinates for cyt *c* Fe(II). For the Mb calculations, we used the coordinates of two recently characterized metalloporphyrins: (*i*-PrNC)(1-methylimidazole)(5,10,15,20-tetraphenylporphinato)Fe(II) and (CO)(1-methylimidazole)(5,10,15,20-tetraphenylporphinato)Fe(II), while literature structures were used for the bis-ligand adducts. We used a "locally dense" basis to evaluate the ^{57}Fe shieldings and electric field gradients at iron and compared them with the measured chemical shifts and Mössbauer quadrupole splittings, respectively. There is moderately good agreement between theory and experiment for the cytochrome *c* and Mb ^{57}Fe chemical shifts and shielding tensors, and very good (0.10 mm s^{-1} rmsd) agreement for the ^{57}Fe Mössbauer quadrupole splittings, using the following basis sets and functional: a Wachters' all electron representation for iron, a 6-311++G(2d) basis for all atoms directly attached to iron, 6-31G* for the second shell and 3-21G* bases for the other more distant atoms, together with a B3LYP hybrid exchange-correlation functional. Extensive tests with other functionals and basis set schemes are also reported. The shift and electric field gradient tensor orientations are generally close to obvious molecular symmetry axes, with the skew of the shielding tensor reversing sign on transition from strong to weak ligand fields. The paramagnetic contribution to shielding overwhelmingly dominates overall shielding and the variations seen between weak ligand field (bis(pyridine), cytochrome *c*) and strong ligand field (CO, PMe_3, *i*-PrNC) systems. Poor accord between theory and experiment is obtained for the ^{57}Fe chemical shifts when MbCO models having highly distorted X-ray geometries are employed, suggesting that the Fe−C−O is close to the porphyrin normal, both in solution and in the solid state.

Introduction

Iron is a major component of most respiratory proteins, acting as both a ligand carrier as well as an electron-transfer catalyst, in systems such as hemoglobin, myoglobin, cytochrome *c*, and ferredoxins.[1] There has therefore been, over the years, considerable interest in studying the structures of these systems, using both diffraction methods as well as spectroscopic techniques. Here, the ^{57}Fe nucleus is a potentially powerful probe of structure/function relationships. There have been numerous studies of the ^{57}Fe Mössbauer spectra of iron porphyrins and proteins,[2,3] and we and others have reported the ^{57}Fe nuclear magnetic resonance (NMR) spectra of several proteins, including ferrocytochrome *c*,[4] carbon monoxy−myoglobin,[5,6] and alkyl isocyanide adducts of myoglobin.[7] However, there has been relatively little progress reported in reproducing, predicting, or analyzing these NMR and Mössbauer parameters and relating them to structure. In early work, Trautwein et al.[8,9] reported the results of iterative extended Hückel calculations of the electric field gradients (efgs) at the iron and hence the ^{57}Fe Mössbauer quadrupole splittings of MbCO, concluding that the Fe−C−O unit was bent at ∼45°, while Case et al.[10] reported promising results for several types of calculations on both CO and O_2 complexes,[10] using a linear and untilted model for MbCO. However, for ^{57}Fe NMR, there have been no reports of the successful prediction of chemical shifts in proteins using quantum chemical techniques, although useful empirical predictions have been made very recently by Walker et al.,[11] based on experimental Mössbauer−NMR correlations.

The principal reasons for this slow progress, which has essentially resulted in only rather qualitative predictions of ^{57}Fe NMR and Mössbauer spectra in proteins, is that ^{57}Fe NMR chemical shift[12] and electric field gradient tensor calculations[13−15]

† This work was supported by the U.S. Public Health Service (National Heart, Lung and Blood Institute grant HL-19481).

‡ Department of Chemistry.

¶ Barry Goldwater Fellow. Present address: Department of Chemistry, University of California, Berkeley, CA.

Swiss National Science Foundation Postdoctoral Research Fellow, 1996−1997; American Heart Association, Inc., Illinois Affiliate, Postdoctoral Research Fellow, 1997−1998.

⊥ Department of Physics.

S1089-5639(97)02542-5 CCC: $15.00
Published on Web 03/07/1998

TABLE 1: Selected Geometric Parameters for Metalloporphyrin DFT Calculations[a]

system	d(Fe−X) (Å)	d(Fe−Y) (Å)	d(Fe−N_{por}) (Å)	∠(X−Fe−Y) (deg)	ref
Fe(OEP)(PMe_3)$_2$	2.2753	2.2753	1.9972	180	25
Fe(TPP)(pyr)$_2$	2.0368	2.0368	2.0008	180	26
Fe(P)(1-MeIm)(Me_2S)	2.3591	2.0246	2.0036	178.3	24
Fe(TPP)(1-MeIm)(^{i}PrNC)	1.8472	2.0426	1.9982	174.1	23
Fe(TPP)(1-MeIm)(CO)	1.7929	2.0699	2.0034	178.2	22

[a] X and Y are the axial ligand atoms coordinated to iron. For PMe_3 and pyr_2, X = Y; for Me_2S, X = S and for *i*-PrNC and CO, X = C.

have become tractable only recently. This is due to recent improvements in computer speed (which enables very large fragments to be investigated), together with the application of density functional theory methods using hybrid exchange-correlation functionals, which enable the rapid and accurate evaluation of both metal ion shifts[12,16,17] as well as electric field gradients,[13−15] at least in model systems, such as metal carbonyls and organometallic compounds. With these improvements in speed and accuracy, it should now be possible to begin to investigate metalloproteins themselves, since both shielding and the efg at the iron nucleus are rather local phenomena, and should not require a detailed knowledge of the rest of the protein's structure, basically the same situation we have found previously, for example, when evaluating amino acid chemical shifts in proteins.[18,19] Here, we therefore investigate the ^{57}Fe NMR shieldings in three proteins whose shifts have been reported previously: ferrocytochrome *c* and the isopropyl isocyanide and carbon monoxide adducts of myoglobin, together with the ^{57}Fe Mössbauer quadrupole splittings in these same proteins, and both the ^{57}Fe NMR shieldings and Mössbauer quadrupole splittings in several other well-defined metalloporphyrins.

Computational Section

Shielding Tensor Calculations. Both chemical shielding and electric field gradient tensor calculations were performed by using the Gaussian 94/DFT program[20] on Silicon Graphics/Cray Origin 200 computers in this laboratory, and on Origin 2000 and Power Challenge Computers located in the National Center for Supercomputing Applications (NCSA) in Urbana, IL. The NMR shielding tensors were calculated using the gauge-including atomic orbital (GIAO) method.[21]

Structures. The structure used for MbCO is a model iron porphyrin, (CO)(1-methylimidazole)(5,10,15,20-tetraphenylporphinato)Fe(II).[22] For the RNC·Mb system, we used as a model (*i*-PrNC)(1-methylimidazole)(5,10,15,20-tetraphenylporphinato)-Fe(II).[23] This compound has a 6° Fe−C tilt from the porphyrin normal and a 10° Fe−C−N bend. For future comparison with experimental solid-state ^{57}Fe shieldings, the phenyl groups were retained in the two tetraphenyl porphyrin (TPP) adducts: Fe-(TPP)(1-MeIm)(CO) and Fe(TPP)(1-MeIm)(*i*-PrNC). The MbCO model calculations were then repeated with three X-ray crystallographic structures of *Physeter catodon* (sperm whale) MbCO reported in the Brookhaven Protein Data Bank (24; Files 1SPE, 1VXC, 1VXF). The structures investigated consisted of the iron porphyrin, minus the alkyl substituents, together with the two axial ligands, all at the crystallographic geometries. For the ferrocytochrome *c* model, we used the same basic structure as with Fe(TPP)(1-MeIm)(CO), except that the CO molecule was replaced by dimethyl sulfide (Me_2S), to mimic the effects of methionine-80 in the protein, and the phenyl groups were replaced with hydrogens. The orientation of the 1-methylimidazole was set to the orientation of His-18 in ferrocytochrome *c*,[24] and the C−S−C coordinates in the Me_2S ligand were superposed on the crystallographic positions for cyt *c* (24; File 1CTJ). Specifically, the Me_2S was "tilted", due to coordination of only one sulfur lone pair to the iron atom. For Fe(OEP)-(PMe_3)$_2$ and Fe(TPP)(pyr)$_2$, literature geometries were used.[25,26] Key geometric information is collected in Table 1.

Basis Sets and Exchange-Correlation Functional. For both shift and efg calculations, we used primarily a locally dense[27] approach in which four sets of basis functions were used. The most dense basis, a Wachters'[28,29] all electron basis (62111111/3311111/3111) was used on iron, a 6-311++G(2d) on all atoms directly coordinated to iron (plus the carbonyl oxygen in MbCO and the N and C in the RNC group), 6-31G* for the next shell, followed by a 3-21G* basis for the most peripheral atoms. The exchange-correlation (XC) functional used was the hybrid B3LYP functional.[20,30,31] SCF energy convergence of these large molecules was carried out in a sequential method by using both Hartree−Fock and density functional theory. In all steps the iron was represented by the Wachters' basis set. For the cytochrome *c* and TPP models, SCF convergence was achieved in the following way. Step 1 was a Hartree−Fock 3-21G* calculation. Step 2 was as in step 1, but the basis sets on the atoms of the first and second shells were replaced by 6-31G*. Step 3 was as in step 2, but with the B3LYP XC functional. Step 4 used the locally dense basis sets/B3LYP calculation. For the MbCO (pH 4−6) crystal models: Step 1 was a 3-21G*/B3LYP calculation. Step 2 was as in step 1, but the 3-21G* basis sets were replaced by 6-31G*. The final step involved property calculations, as in Step 4 above**.** For cytochrome *c* (570 basis functions), isopropyl isocyanide (866 basis functions) and carbon monoxy (784 basis functions) myoglobin models, the timings over 16 CPUs were 8, 21 and 13 h, respectively, on Origin 2000 computers. Similar schemes were also used for the bis(PMe_3) and bis(pyr) adducts. We also carried out a series of additional shielding and efg calculations in which the effects of functional, basis set size, as well as geometric structure, were modified, as discussed in detail below.

Experimental Section

Methyl and propyl isocyanide adducts of ^{57}Fe-enriched sperm whale myoglobin were made basically as described previously.[7] Mössbauer spectra were obtained using a "home-built" constant acceleration spectrometer. Protein samples were investigated as frozen glasses at 77 K, while model compounds were measured in polycrystalline form, also at 77 K.

Results and Discussion

As noted above, there exists some controversy as to the details of the active site structures of heme proteins. It would therefore be helpful if it were possible to accurately correlate in some way spectroscopic observations to structural features with the long-term goal of refining or even predicting aspects of protein structure. Here, modern Kohn−Sham density functional theory offers some promise for making the required nexus between spectra and structure. In this work, we present our initial results

TABLE 2: ^{57}Fe NMR Shielding for Heme Model Compounds and Shift and Shift Anisotropy Data for Heme Proteins[a]

system	shielding tensor element σ_{11}(ppm)	σ_{22}(ppm)	σ_{33}(ppm)	isotropic shielding σ_i(ppm)	isotropic shift[b] δ_i (ppm) calc[b]	expt	tensor span, Ω $\lvert\sigma_{33} - \sigma_{11}\rvert$ (ppm) calc	expt
Fe(P)(PMe_3)$_2$	−10 414	−10 285	−10 066	−10 255	7 343	7 873	348	NM
Fe(P)(pyr)$_2$	−16 674	−15 835	−11 413	−14 641	11 729	11 723	5 261	NM
Fe(P)(1-MeIm)(Me_2S)/cyt *c*	−17 053	−16 707	−11 038	−14 933	12 021	11 197[c]	6 015	7630[c]
Fe(TPP)(1-MeIm)(*i*-PrNC)/Mb·RNC	−11 431	−11 112	−10 994	−11 179	8 267	9 257[d]	437	1260[d]
Fe(TPP)(1-MeIm)(CO)/MbCO	−11 712	−10 330	−9 968	−10 670	7 758	8 227[e]	1 744	3600[f]
MbCO, pH 4	−27 310	−16 978	−9 331	−17 873	14 961	8 227[e]	17 979	3600[f]
MbCO, pH 5	−21 805	−17 506	−9 878	−16 397	13 485	8 227[e]	11 927	3600[f]
MbCO, pH 6	−19 886	−18 278	−10 003	−16 056	13 144	8 227[e]	9 883	3600[f]

[a] Evaluated using the locally dense basis/B3LYP DFT method described in the text. [b]The isotropic shifts are obtained from the computed absolute shieldings using δ (shift, ppm) = −2912 − σ (calc, ppm). The −2912-ppm value comes from the intercept shown in Figure 1 and is approximately the computed absolute shielding of Fe(CO)$_5$, the experimental ^{57}Fe NMR chemical shift standard, taken to be at 0 ppm. [c] cyt *c*, ref 4. [d] *n*-PrNC·Mb, ref 7. [e] MbCO, refs 5 and 6. [f] MbCO, ref 5.

on using the ^{57}Fe nucleus as a structure probe, both in solution (NMR) and in the solid state (Mössbauer). By investigating the ^{57}Fe chemical shifts, the ^{57}Fe shielding tensor elements, as well as the ^{57}Fe Mössbauer quadrupole splittings in different model systems, and comparing these results with experimental results on metalloporphyrins (whose structures are accurately know) and on proteins (RNC·Mb, MbCO, and cyt *c* (FeII)), we can begin to investigate to what extent metal ion shifts and electric field gradients (which are related to the Mössbauer quadrupole splittings, ΔE_Q) can now be predicted in proteins, using modern theoretical methods. In addition, we can begin to test ideas about how specific, (computer) engineered distortions, might be expected to affect the spectroscopic observables. As with our work on amino acid conformations in peptides and proteins,[32,33] the hope is that this should then lead to methods to predict and refine local metal−ligand structure in metalloproteins, as well as provide interesting information on local electronic structure, and thereby on function.

We show in Table 2 the ^{57}Fe nuclear magnetic resonance shielding tensor elements, σ_{11}, σ_{22}, and σ_{33}, and the isotropic spectroscopic shieldings we have calculated for the bis(PMe_3) and bis(pyr) metalloporphyrin systems, as well as for the ferrocytochrome *c* model, the *i*-PrNC, and (linear) MbCO model compounds. These results are compared with experiment in Figure 1 and in Table 2. For purposes of comparison, we first consider the isotropic shieldings for these five systems, together with the shifts of a series of iron carbonyls and ferrocene previously reported by Bühl.[12] In this pioneering study, Bühl found good agreement between predicted and experimental ^{57}Fe NMR chemical shifts,[12] with a slope of −0.965 and an R^2 value of 0.979 being obtained, together with a shielding intercept (0 ppm shift) for Fe(CO)$_5$ of −2961 ppm and a mean absolute error between experiment and theory of 84 ppm, at the GIAO−B3LYP level, using a similar basis set to that which we have used. When the five metalloporphyrin/metalloprotein results are added to his correlation (Figure 1A), we find an overall slope of −0.984, an R^2 value of 0.992, and an intercept of −2912 ppm. The mean absolute errors for the protein model calculations are, however, much larger than with the metal carbonyls and metalloporphyrins, Table 1, which is not unexpected since the exact structures of the proteins are not known. Nevertheless, we believe these results do indicate moderately good agreement between calculation and experiment, Figure 1A, implying that it should now be possible to begin to investigate iron shifts/shieldings in other metalloporphyrins and metalloproteins, using similar methods.

It is also possible that the agreement between theory and experiment may actually be rather better than these results indicate. Specifically, Baltzer and Landegren[34] have reported

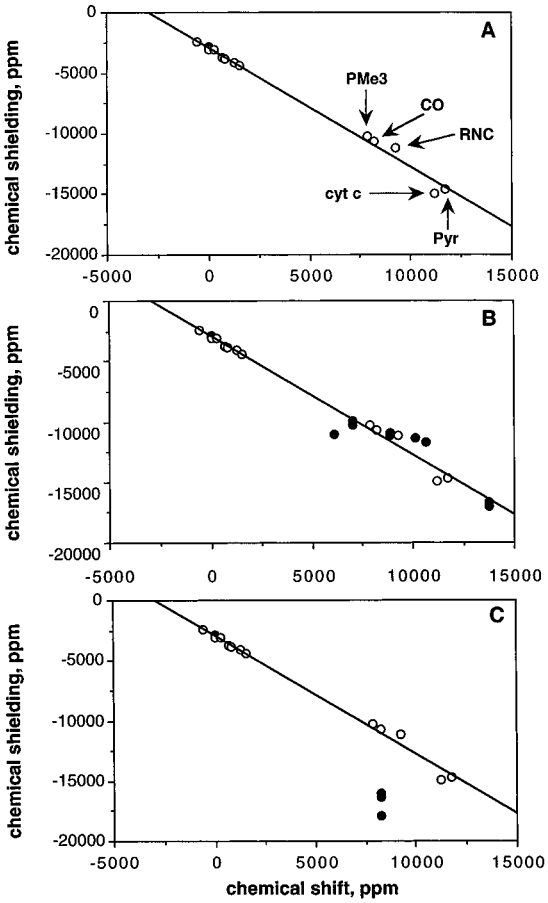

Figure 1. Experimental versus computed ^{57}Fe nuclear magnetic resonance chemical shifts and chemical shieldings for ferrocytochrome *c*, RNC·Mb, MbCO, and several model compounds. (A) Experimental chemical shifts versus calculated isotropic shieldings. The points in the top left corner are all from ref 12. The bis-PMe_3, bis-pyr, ferrocytochrome *c*, RNC·Mb, and MbCO shieldings are indicated. (B) As in (A) but the shielding tensor elements for cyt *c*, RNC·Mb, and MbCO, as estimated from solution T_1 measurements, are also shown (●). (C) As in (A) but the isotropic shieldings based on three MbCO crystal structures (ref 39) are also shown. The overall slope in (A) for all points is −0.984, with an intercept of −2912 ppm and an R^2 value of 0.992.

the results of a series of ^{57}Fe NMR chemical shift measurements on a range of porphyrins having ruffled structures, due to steric constraints. The chemical shifts they observe are all more shielded than we find experimentally for MbCO in solution.[5,34] For example, with increased ruffling, the shifts decrease from 8036 to 7500 ppm (from Fe(CO)$_5$) in a basket handle porphyrin.[34] The computed isotropic chemical shift of 7760 ppm

TABLE 3: ^{57}Fe Shielding Tensor Calculations for Model Iron (CO)(1-methylimidazole) Porphyrins as a Function of Molecular Structure, Basis Sets, and Exchange-Correlation Functionals

system[a]	structure[b]	XC[c]	basis sets	σ_i (ppm)	σ_{11} (ppm)	σ_{22} (ppm)	σ_{33} (ppm)
1. Fe TPP	riding[b]	B3LYP	Wachters/6-311++G(2d) CO&N/6-31G* Cα/3-21G* others	−10 670	−11 712	−10 330	−9 968
2. Fe TPP	opt[b]	B3LYP	Wachters/6-311++G(2d) CO&N/6-31G* Cα/3-21G* others	−10 868	−11 819	−10 558	−10 227
3. Fe TPP	opt[b]	BPW91	Wachters/6-311++G(2d) CO&N/6-31G* Cα/3-21G* others	−7 532	−7 710	−7 500	−7 387
4. Fe TPP	riding	BPW91	Wachters/6-311++G(2d) CO&N/6-31G* Cα/3-21G* others	−7 388	−7 581	−7 357	−7 227
5. Fe P	riding[a]	BPW91	Wachters/6-311++G(2d) CO&N/6-31G* Cα/3-21G* others	−7 394	−7 596	−7 366	−7 220
6. Fe P	riding[a]	BPW91	Wachters/6-311++G(2d) CO&N/6-31G* porphyrin ring/3-21G* H	−7 410	−7 620	−7 380	−7 232
7. Fe P	X-ray[c]	BPW91	Wachters/6-311++G(2d) CO&N/6-31G* Cα/3-21G* others	−7 360	−7 546	−7 316	−7 216

[a] Fe TPP = four phenyl groups were incorporated in the calculations; Fe P = iron porphyrinate structure in which meso substituents were replaced by hydrogens. [b] Riding = a riding model geometry optimized X-ray structure (ref 22) was used: d(C−O) = 1.094 Å and d(Fe−C) = 1.793 Å. Opt = a DFT constrained (d(Fe−C), d(C−O)) geometry optimized structure was used in which d(C−O) = 1.149 Å and d(Fe−C) = 1.805 Å (ref 22). X-ray = the X-ray structure (ref 22) in which d(C−O) = 1.061 Å and d(Fe−C) = 1.793 Å were used.

(Table 2) is well within the range of 7500−8036 reported by Baltzer and Landegren for their ruffled iron porphyrins containing CO and alkylimidazole ligands.[34] Thus, since the degree of ruffle in the protein is uncertain, while a saddle distortion is seen in the model system,[22] the possibility exists that part of the error seen in the calculations originates from a porphyrin ring distortion. Solid-state ^{57}Fe NMR results will be required in order to explore this possibility further.

To test the sensitivity of the shielding calculations to structural effects, as well as the effects of basis set size and the type of XC functional used, we also carried out an additional series of calculations on (CO)(1-MeIm)(TPP)Fe(II), the MbCO model system. Shielding results are given in Table 3. As expected, choice of functional has the major effect on the isotropic shielding (**2**, **3**). Changes in local geometry, such as a change in the C−O bond length, have only a modest effect on shielding (**1**, **2, 7**), while replacement of phenyl groups by hydrogens has essentially no effect (**4**, **5**). The iron shieldings are also only moderately sensitive to the details of the locally dense basis set schemes employed, as can be seen in Table 3 (**5**, **6**). However, it should be noted that only the hybrid B3LYP XC functional gives a large tensor span. For the riding model geometry optimization, we find $\Delta\sigma$ = 1744 ppm with the B3LYP functional, while all of the BPW91 calculations yield very small values, on average only ∼350 ppm, about 10% of that estimated from experiment.[5] Consequently, we have used the B3LYP functional for most shielding calculations, and, as we show below, moderately good accord between theory and experimental tensor spans are obtained when a series of porphyrins are investigated.

For the ferrocytochrome *c* model system, we calculate an isotropic chemical shift of 12 021 ppm from $Fe(CO)_5$, which is to be compared with the experimental result published by Baltzer[4] of 11 197 ppm from $Fe(CO)_5$, where in both cases we have used the intercept of −2912 ppm (the absolute isotropic shielding of $Fe(CO)_5$ corresponding to a 0 ppm chemical shift, evaluated from the intercept in Figure 1A), that is:

$$\delta\ (\text{ppm, Fe(CO)}_5) = -2912 - \sigma\ (\text{ppm, absolute shielding}) \quad (1)$$

Clearly, the iron atom in ferrocytochrome *c* is considerably more deshielded than is observed in the PMe_3, MbCO, and *i*-PrNC model systems, at least at the MbCO model geometry (linear and untilted Fe−C−O) we have used, and is very close to the shifts/shieldings seen for the bis(pyridine) adduct, Table 2. As we shall see below, this large change in isotropic shift in the ferrocytochrome *c* model is also accompanied by a large change in the shift anisotropy, as reported by Baltzer.[4]

For ferrocytochrome *c*, MbCO, and RNC·Mb, we and others have previously made estimates of the ^{57}Fe chemical shift anisotropy (CSA), based on T_1 measurements. The spin−lattice relaxation rate of iron-57 appears to be dominated by the chemical shift anisotropy relaxation mechanism,[5,7] in which case:

$$1/T_1 = (1/15)\gamma^2 H_0^2(\delta_\perp - \delta_{||})^2 \frac{2\tau_R}{1 + \omega^2\tau_R^2} \quad (2)$$

where $(\delta_\perp - \delta_{||})$ is the overall span of the shielding tensor. This assumes axial symmetry, a not unreasonable assumption which is borne out, in most cases, from the results of the calculations, Table 2. In our previous work, we reported two possible sets of solutions for $\delta_\perp$, $\delta_{||}$, since clearly the sign of $(\delta_\perp - \delta_{||})$ cannot be deduced from the relaxation measurements, because the CSA appears as $(\delta_\perp - \delta_{||})^2$, eq 2. The results of the theoretical calculations clarify the sign question, Table 2, and enable a comparison between the experimental results for the shielding tensor elements (assuming axial symmetry as was done previously) and the theoretical predictions. These results are shown in Figure 1B (solid circles, ●). There is clearly less good accord between theory and experiment for the tensor elements than for the isotropic shifts alone. This can be attributed in large part to the difficulty of determining accurate shift anisotropies from solution T_1 and line width measurements.

These theoretical calculations of the ^{57}Fe shielding tensor, together with the corrected value of the ^{57}Fe shielding in Fe(TPP)$(pyr)_2$,[11] now permit a revised interpretation of the shielding tensors, and their orientations, in both metalloporphyrins and metalloproteins as well.

As can be seen in Table 2 and in Figure 2, there is a large range of ^{57}Fe NMR shielding observed for metalloporphyrins and metalloproteins. In the Fe(TPP)$(pyr)_2$ system, the shielding tensor is close to axially symmetric, with both σ_{11} and σ_{22} being highly deshielded and oriented in the plane of the porphyrin, Figure 3A. Essentially the same tensor orientation and magnitude is also seen with the ferrocytochrome *c* model, Figure 3B, with σ_{33} oriented along the porphyrin normal in both cases. The large deshielding is associated with the small $\Delta E(^1\text{E})\ d_{z^2} \leftarrow (d_{xz}, d_{yz})$ transitions, perpendicular to the heme plane, resulting in large deshieldings of the in-plane elements, σ_{11} and σ_{22}.

In sharp contrast, in MbCO, the much stronger ligand field of CO results in substantially less paramagnetic and overall shielding, Table 4, so much so that the in-plane elements become even more shielded than the unique element, perpendicular to the porphyrin plane, Figures 2 and 3C. That is, the tensor remains close to axially symmetric, but now σ_{11} is unique, and $\sigma_{22} \sim \sigma_{33}$ and both appear at very high field. The tensor thus changes sign (or skew) on transition from a weak to a strong ligand field. While this is, of course, a rather pictorial description, the theoretical shielding tensor values, and their

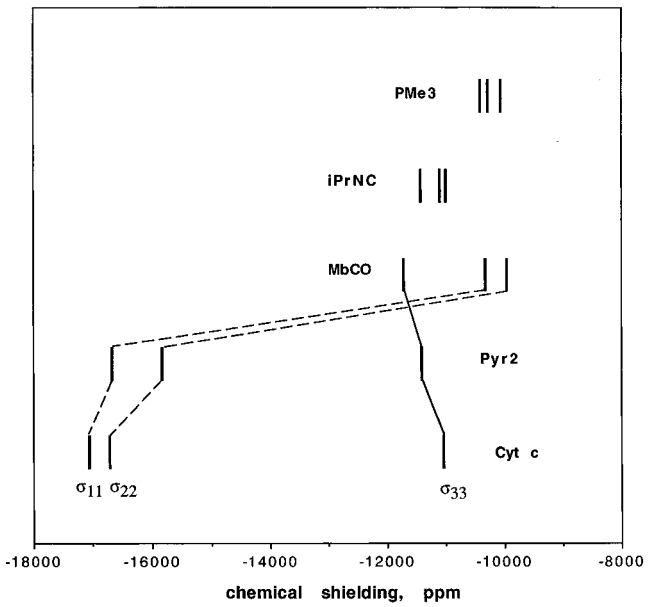

Figure 2. Values for principal components of the ^{57}Fe NMR shielding tensors in the systems indicated. The tensor components clearly perpendicular to the unique axis (i.e., those in the heme plane) are connected by dotted lines. The tensor components parallel to the unique axis (i.e., those along the heme normal) are connected by solid lines. The *x*-axis represents the total computed absolute shielding, and $\sigma_{33} > \sigma_{22} > \sigma_{11}$. The stick diagram would look the same using the standard δ-scale chemical shift convention, with the most deshielded element, δ_{11}, being to the left.

orientations, now permit a revision of previous ideas,[4,7,11] which were based in large part on the erroneous shift values for Fe(TPP)(pyr)$_2$.

The Fe(TPP)(pyr)$_2$, ferrocytochrome *c*, and MbCO ^{57}Fe shielding tensors are all close to axially symmetric, with the unique axis perpendicular to the heme normal. This value (σ_{33} in Fe(TPP)(pyr)$_2$ and cyt *c*, σ_{11} in MbCO) changes little from system to system, while the in-plane elements (σ_{11} and σ_{22} in Fe(TPP)(pyr)$_2$ and cyt *c*, σ_{22} and σ_{33} in MbCO) dominate the overall shieldings changes seen. When the in-plane elements track to high field (on increasing the ligand field splitting with stronger π-acceptor ligands, like RNC, PR$_3$), then the situation $\sigma_{11} \sim \sigma_{22} \sim \sigma_{33}$ can occur, and a very small shift anisotropy may be observed. This is clearly the case with PMe$_3$ and *i*-PrNC in Fe(TPP)(1-MeIm)(PMe$_3$)$_3$ and *i*-PrNC·Mb, and results in the latter case in a very long solution T_1 value.[7] In the case of the Fe(TPP)(1-MeIm)(*i*-PrNC) model system calculation, the tensor is actually somewhat asymmetric, Figure 3D, due presumably to the fact that the *i*-PrNC group is somewhat tilted and bent (the total tilt and bend is 16°). The distortions in the CO adduct are much less (<2°), and the tensor is more symmetric. As noted previously,[11] the paramagnetic contribution to shielding overwhelmingly dominates the total absolute shielding, Table 4, and variations in σ_p control the observed shifts seen experimentally.

These ^{57}Fe chemical shift/shielding calculations therefore indicate the following. There is moderately good accord between theory and experiment for the ^{57}Fe shifts in metalloporphyrins and metalloproteins. The correct ordering of the ^{57}Fe chemical shifts in three proteins is obtained: δ_i (cyt *c*) $\gg$ δ_i(RNC·Mb) > δ_i(MbCO). The correct ordering of $\Delta\sigma$ is also obtained: $\Delta\sigma$(cyt *c*) $\gg$ $\Delta\sigma$(MbCO) > $\Delta\sigma$(RNC·Mb). The experimental $\Delta\sigma$ for cytochrome *c* was reported by Baltzer to be 7630 ppm, while we predict $\Delta\sigma$ = 6015 ppm, good agreement when considering the uncertainties associated with the structural model, in which the Fe−N$_{im}$ and Fe−S distances were based on the protein crystal structure, and the experimental errors associated with the determination of $\Delta\sigma$. In addition, a small $\Delta\sigma$ for the RNC adducts also emerges from the calculations, consistent with the long T_1 values seen experimentally.[7] And finally, all five porphyrin and protein points lie on and extend by ~9000 ppm the small molecule correlation previously established by Bühl.[12]

Next, we show in Table 2 and Figure 1C the results of ^{57}Fe NMR shielding calculations based on numerous reports[35−39] of highly distorted geometries in MbCO, both in the crystalline solid state and in solution. Using the most recent crystallographic structures,[39] differences between experiment and calculation of ~5000−7000 ppm are observed, Table 2 and Figure 1C. One possibility for these differences might be that the solution and crystal structures are very different. Another might be that more accurate crystallographic structures are needed in order to reproduce the experimental chemical shifts. A third is that the calculations themselves are in error. However, the results of recent solution infrared spectroscopic measurements also imply a <7° Fe−CO tilt in solution,[40] consistent with the good correlation we find using a model compound with linear, untilted FeCO. Single-crystal IR measurements also imply only a very small distortion in sperm whale $P2_1$ crystals as well,[41] again consistent with the second possibility mentioned above, and recent DFT calculations which explore the relationships between IR and ligand NMR shielding also conclude a close to linear and untilted Fe−C−O fragment in most heme proteins.[42]

Finally, we briefly report the results of our electric field gradient tensor (Mössbauer quadrupole splitting) calculations at iron in metalloporphyrin and metalloprotein model systems. The goal here is to determine whether Mössbauer quadrupole splittings, ΔE_Q, can be reliably evaluated for metalloproteins using the same structures/basis sets/functional as used for the ^{57}Fe shift calculations. The Mössbauer quadrupole splitting is related to the components of the electric field gradient tensor as follows:

$$\Delta E_Q = \frac{1}{2} e Q V_{zz} \left(1 + \frac{\eta^2}{3}\right)^{1/2} \tag{3}$$

where *e* is the electron charge, *Q* the quadrupole moment of the $I^* = 14.4$ keV excited state, and the components of the efg are labeled according to the convention:

$$|V_{zz}| > |V_{yy}| > |V_{xx}| \tag{4}$$

with the asymmetry parameter

$$\eta = (V_{xx} - V_{yy})/V_{zz} \tag{5}$$

In separate work,[43] we have found good accord (~0.2 mm s^{-1} rmsd) between experimental and computed ΔE_Q values for a series of organometallic compounds by using a quadrupole moment, *Q*, of 0.16×10^{-28} m^2.[44] In addition, we have also recently carried out a second set of ^{57}Fe shift and Mössbauer ΔE_Q calculations to investigate in even more detail the effects of functional on the computed results. Here, we used as a model a geometry optimized Fe(CO)$_5$ structure (Fe LANL2DZ ECP/basis, 6-31G* on C and O, BP86 exchange-correlation functional in Gaussian 94) using Wachters' all electron basis on iron, and 6-311++G(2d) on C and O. The results obtained with eight different functionals are given in Table 5. Clearly, the Becke

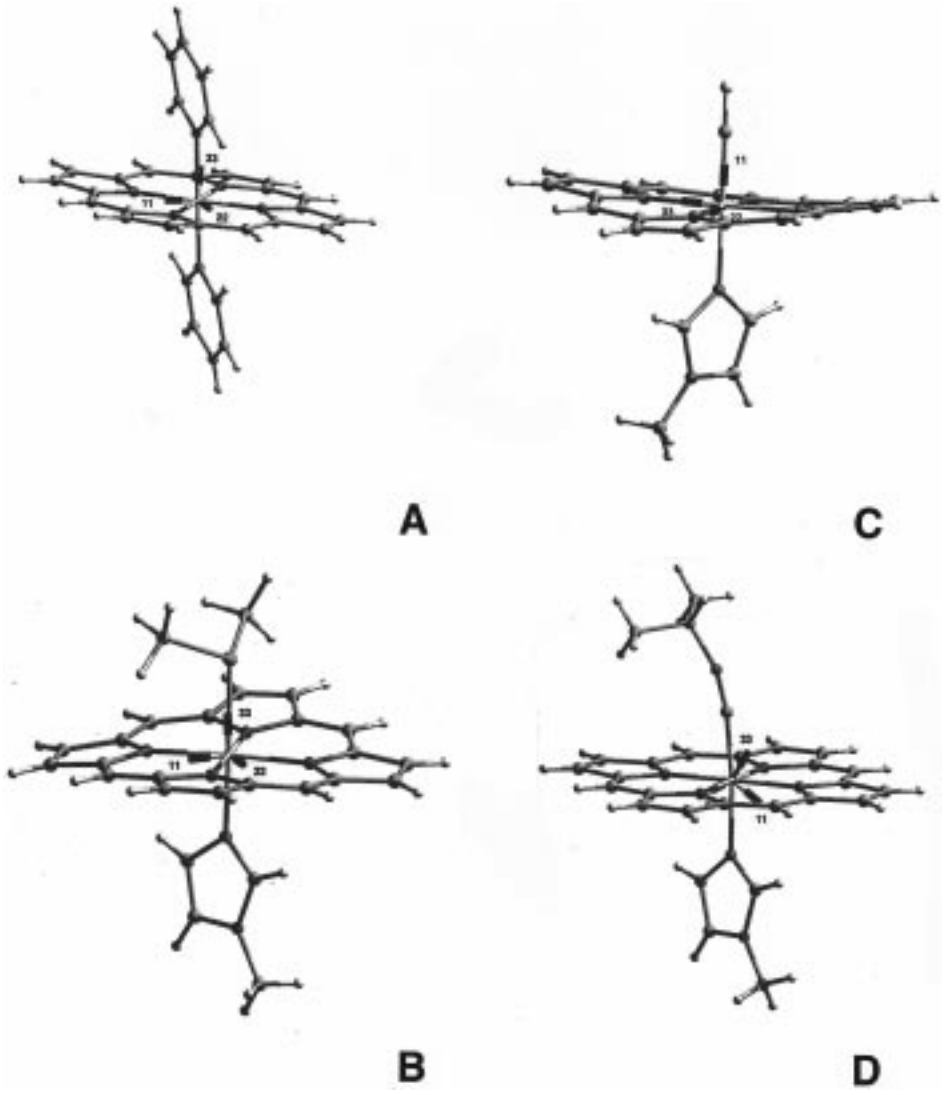

Figure 3. Orientations of the principal components of the ^{57}Fe NMR shielding tensor (σ_{ii}, computed) for metalloporphyrin and metalloprotein model systems: (A) Fe(P)(pyr)$_2$, (B) Fe(P)(1-MeIm)(Me$_2$S), (C) Fe(TPP)(1-MeIm)(CO), (D) Fe(TPP)(1-MeIm)(*i*-PrNC). The phenyl substituents have been removed for clarity.

TABLE 4: Diamagnetic and Paramagnetic Contributions to Shielding in Metalloporphyrin and Metalloprotein Model Systems[a]

system	shielding (ppm)		
	σ_{dia}	σ_{para}	σ_{total}
Fe(P)(PMe$_3$)$_2$	2018	−12 273	−10 255
Fe(TPP)(pyr)$_2$	2038	−16 678	−14 640
Fe(TPP)(1-MeIm(Me$_2$S)	2025	−16 958	−14 933
Fe(TPP)(1-MeIm)(*i*-PrNC)	2018	−13 197	−11 179
Fe(TPP)(1-MeIm)(CO)	2016	−12 686	−10 670

[a] Computed using the Gaussian 94 program using a Wachters' all electron basis for iron and a B3LYP hybrid exchange correlation functional, as described in the text.

three-parameter hybrid functionals B3LYP, B3P86, and B3PW91 give good accord with the experimental Mössbauer ΔE_Q (2.51 mm s^{-1}) supporting their use in such calculations. Moreover, the computed absolute NMR shielding in all three cases is close to the Fe(CO)$_5$ intercept (of −2912 ppm) deduced from the correlation shown in Figure 1A, with, as expected, the B3LYP functional yielding closest agreement. The pure density functionals BLYP and BP86, and the BHandH and BHandHLYP functionals,[20] perform noticeably poorer for ΔE_Q and σ, and were thus not explored further.

TABLE 5: Effects of Functional on ^{57}Fe Isotropic Shielding and on the Mössbauer ΔE_Q in Fe(CO)$_5$

functional[a]	σ_i (ppm)	ΔE_Q (mm s^{-1})
B3LYP	−2895.2	2.55
BLYP	−2036.9	2.22
BP86	−1931.4	2.20
BPW91	−1940.8	2.21
B3P86	−2784.6	2.55
B3PW91	−2785.9	2.55
BHandH	−4680.4	2.83
BHandHLYP	−4852.2	2.85
expt	−2912[b]	2.51

[a] For a more detailed description of each functional, see, e.g., ref 20. [b] Obtained from eq 1.

In Table 6 we compare the results of ^{57}Fe efg calculations for three porphyrins and three protein models with experimental data. The three metalloporphyrins are the bis(PMe$_3$) and bis-(1-MeIm) complexes recently studied both theoretically and experimentally by Grodzicki et al.,[45] and the bis(pyr) complex of tetraphenylporphyrin.[46] For the three model systems, there is excellent accord with experiment (0.12 mm s^{-1} error in ΔE_Q, without use of any Sternheimer factor) using the same basis sets and functional as we used for the ^{57}Fe NMR shielding calculations, which gives additional confidence in the quality

TABLE 6: Eigenvalues of the Electric Field Gradient Tensors for ^{57}Fe in Metalloporphyrins, Ferrocytochrome *c*, *i*-PrNC·Mb and MbCO Model Compounds Together with Computed and Experimental Protein Mössbauer Quadrupole Splittings[a]

	electric field gradient tensor elements			quadrupole splittings ΔE_Q(mm s^{-1})[b]		asymmetry parameter η	
system	q_{zz} (au)	q_{xx} (au)	q_{yy} (au)	calc	expt	calc	expt
Fe(TPP)(pyr)$_2$	−0.682	0.296	0.386	1.11	1.15	0.14	NM
Fe(TMP)(NMeIm)$_2$	−0.613	0.220	0.393	0.99	1.07	0.28	0.0 (1)
Fe(OEP)(PMe$_3$)$_2$	−0.062	0.028	0.034	0.10	0.35	0.10	0.6 (1)
FeP(NMeIm)(Me$_2$S)	−0.805	0.327	0.479	1.31	1.20[c]	0.19	∼0.5[d]
Fe(TPP)(NMeIm)(*i*-PrNC)	−0.200	0.086	0.112	0.33	0.33−0.40[e]	0.13	NM
Fe(TPP)(NMeIm)(CO)	−0.269	0.110	0.159	0.44	0.36−0.37[f]	0.18	<0.4−0.75[f]

[a] Computed using the locally dense basis set approach and the B3LYP hybrid exchange-correlation functional, as described in the text. [b] An ^{57}Fe^{m}quadrupole moment of 0.16 × 10^{-28} m^2 was used, ref 44. [c] Value reported for horse heart ferrocytochrome *c* in ref 47. [d] Reference 3. [e]Values for MeNC·Mb (0.40 mm s^{-1}) and *i*-PrNC·TPP model (0.33 mm s^{-1}), see Figure 4. [f] Values reported for sperm whale carbon monoxy−myoglobin from refs 8 and 48.

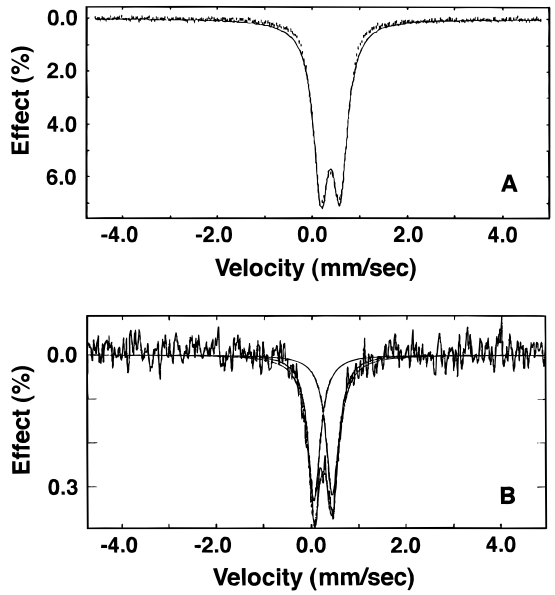

Figure 4. (A) ^{57}Fe Mössbauer spectrum and simulation of MeNC·Mb in frozen solution, 77 K. (B) ^{57}Fe Mössbauer spectrum and simulation of polycrystalline Fe(TPP)(1-MeIm)(*i*-PrNC), 77 K.

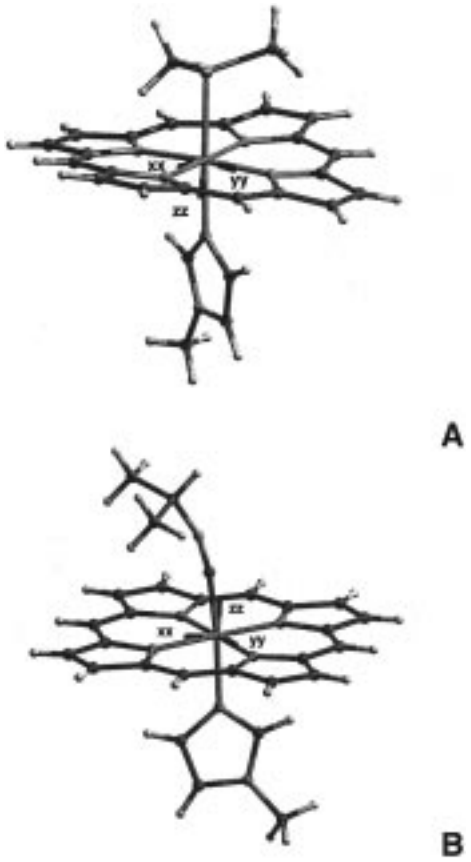

Figure 5. Orientations of the ^{57}Fe electric field gradient tensor: (A) ferrocytochrome *c*, (B) an *i*-PrNC·Mb model. Porphyrin substituents in B have been removed for clarity.

of the calculations. In all cases the sign of the dominant efg component is found to be negative, implying a positive quadrupole interaction, $\Delta E_Q > 0$, and the asymmetry is relatively small, $\eta \approx 0.2$. For ferrocytochrome *c* the calculation yields a Mössbauer quadrupole splitting of 1.31 mm s^{-1}, in very good agreement with the experimental result, $\Delta E_Q = 1.2$ mm s^{-1}.[47] Similarly good agreement is obtained for the *i*-PrNC·Mb model system, in which a ΔE_Q value of 0.33 mm s^{-1} is obtained, to be compared with experimental ΔE_Q values of 0.40 mm s^{-1} for MeNC·Mb, Figure 4A, 0.33 mm s^{-1} for *n*-PrNC·Mb and 0.39 mm s^{-1} for Fe(TPP)(1-MeIm)(*i*-PrNC), Figure 4B. The MbCO model system also shows good agreement with experiment (0.44 mm s^{-1} calculated versus the experimental value of ∼0.36−0.37 mm s^{-1} for MbCO[8,48]). Both results are within the expected ∼0.2 mm s^{-1} rms error found for a series of model compounds, as described elsewhere,[43] and in all cases V_{zz} is oriented close to the porphyrin normal, Figure 5.

Lacking high-field Mössbauer data for the RNC myoglobins, the sign of ΔE_Q in these compounds is not known, although the correct signs for the other systems are in accord with experiment. However, since the isocyanides are isoelectronic with the CO derivatives, which have $\Delta E_Q > 0$, it is plausible to assume the same sign for the isocyanides, which then agrees with the model calculations. This then implies an rms error of only 0.10 mm s^{-1} for the theory-versus-experiment correlation for these three metalloporphyrins and three metalloproteins. This is a very small error indeed, obtained without use of any adjustable parameters, so there is considerable hope for using Mössbauer ΔE_Q values in more detailed structural studies, as we will describe elsewhere.[49] What is puzzling about our results, however, is the poor accord between the experimental and computed η values. Our η values for the model systems are in good accord with the theoretical values reported by Grodzicki et al.,[45] and it is unclear why V_{zz} and the ^{57}Fe NMR isotropic shift would be so well reproduced, while V_{xx} and V_{yy} would be inaccurate — and the same in both sets of calculations. One possibility is that the experimental η values are less accurate than thought, due e.g. to slight magnetic alignment, and certainly the large range in η reported for MbCO (from <0.4 to 0.75, see ref 48) would suggest some type of experimental origin.

Thus both ^{57}Fe NMR chemical shieldings as well as ^{57}Fe Mössbauer quadrupole splittings for ferrocytochrome *c* and two

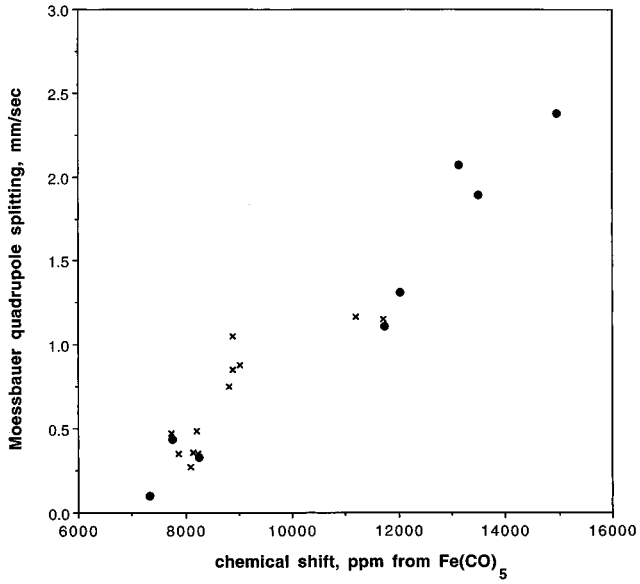

Figure 6. Graph showing correlations between ^{57}Fe NMR chemical shifts and ^{57}Fe Mössbauer quadrupole splittings: (×) experimental results from ref 11, (●), computed values from Tables 2 and 6 and unpublished results on pH 4, 5, and 6 MbCO (ref 43).

myoglobins, as well as several metalloporphyrins, can now be predicted with reasonable accuracy by use of modern density functional theory. This enables the empirical correlations between ^{57}Fe NMR chemical shifts and Mössbauer ΔE_Q values to be put on a more quantitative theoretical footing, and a compilation of NMR shift and Mössbauer quadrupole splitting results determined experimentally,[11] together with those we have calculated theoretically, are shown in Figure 6. While there is a generally linear relationship between δ (NMR) and ΔE_Q (Mössbauer), it is perhaps worth emphasizing that a perfectly linear relation is not expected theoretically, since the efg depends only on the ground state of the system, while both ground state and excited states are important for shielding. Such a correlation is nevertheless of interest since, e.g., it shows that highly distorted MbCO systems having large ΔE_Q and δ values (which are not seen experimentally) fall on the same δ, ΔE_Q correlation as those which are seen experimentally, and which are reproduced theoretically using close to linear and untilted Fe−C−O porphyrin models.

Since there are many iron-containing metalloproteins in which structural questions exist, these results suggest that quantum chemical methods are now at the point where such questions can begin to be answered in a routine manner. Moreover, as more and more correlations are made, it should be possible to combine the results of different spectroscopic techniques to enable even more accurate tests of structure, by using, for example, a combination of NMR and Mössbauer spectroscopy to predict metal−ligand geometries[49] via the Bayesian probability methods described elsewhere for peptide backbone structure prediction.[32,33] Such tests have now, in fact, been performed and confirm the close to linear and untilted model for Fe−C−O in MbCO discussed above.[49]

Conclusions

The results we have described above are of interest since they demonstrate that ^{57}Fe NMR shifts and Mössbauer quadrupole splittings in metalloporphyrin and metalloprotein systems (ferrocytochrome *c*, isopropyl isocyanide−myoglobin, and carbon monoxy−myoglobin) can now be predicted by density functional theory with locally dense basis sets and a hybrid exchange−correlation functional, using metalloporphyrin structures. The correct ordering of isotropic shifts as well as the correct ordering of the shift anisotropies is obtained with the proteins, with the cytochrome *c* anisotropy being exceptionally large, ∼6000 ppm, consistent with previous experimental estimates. The overall rms error for the protein isotropic shifts of ∼800 ppm is relatively large, however, probably due to residual structural uncertainties, such as porphyrin ruffling. Notably, however, the highly distorted CO ligand geometries reported in some studies lead to resonances predicted to be ∼6000 ppm deshielded from experiment. The ^{57}Fe Mössbauer quadrupole splittings have an rms error between theory and experiment of only ∼0.1 mm s^{-1}, and correctly reproduce for the first time the relatively large ΔE_Q value for ferrocytochrome *c*, and the very small ΔE_Q values for the RNC and CO adducts of Mb seen experimentally. Such methods should therefore now be applicable to analyzing the broad base of ^{57}Fe Mössbauer data, and, when combined together, the joint application of ^{57}Fe NMR and Mössbauer measurements may enable the solution of numerous questions related to metalloprotein structure, and potentially structure/function relations as well. Theoretical studies of the ^{57}Fe Mössbauer spectra of paramagnetic metalloproteins, unusual bonding situations such as Fe(IV)O, as well as other nuclei, such as ^{61}Ni and ^{67}Zn, also now appear tractable.

Acknowledgment. This work was supported in part by use of the SGI/Cray Origin 2000 and Power Challenge clusters at the National Center for Supercomputing Applications (funded in part by the U.S. National Science Foundation Grant CHE-97002ON).

References and Notes

(1) Stryer, L. *Biochemistry* Freeman: San Francisco, 1988.

(2) Sams, J. R.; Tsin, T. B. In *The Porphyrins*; Dolphin, D., Ed.; Academic Press: New York, 1979; Vol. 4, pp 425−478.

(3) Debrunner, P. G. In *Iron Porphyrins*; Lever, A. B. P., Gray, H. B., Eds.; VCH Publishers: New York, 1989; Vol. 3, pp 139−234.

(4) Baltzer, L. *J. Am. Chem. Soc.* **1987**, *109*, 3479−3481.

(5) Lee, H. C.; Gard, J. K.; Brown, T. L.; Oldfield, E. *J. Am. Chem. Soc.* **1985**, *107*, 4087−4088.

(6) LaMar, G. N.; Dellinger, C. M.; Sankar, S. S. *Biochem. Biophys. Res. Commun.* **1985**, *128*, 628−633; Baltzer, L.; Becker, E. D.; Tschudin, R. G.; Gansow, O. A. *J. Chem. Soc., Chem. Commun.* **1985**, 1040−1041.

(7) Chung, J.; Lee, H. C.; Oldfield, E. *J. Magn. Reson.* **1990**, *90*, 148−157.

(8) Trautwein, A.; Maeda, Y.; Harris, F. E.; Formanek, H. *Theor. Chim. Acta* **1974**, *36*, 67−76.

(9) Trautwein, A. In *Structure and Bonding*; Dunitz, J. D., Hemmerich, P., Holm, R. H., Ibers, J. A., Jørgensen, C. K., Neilands, J. B., Reinen, D., Williams, R. J. P., Eds.; Springer-Verlag: New York, 1974; pp 101−167.

(10) Case, D. A.; Huynh, B. H.; Karplus, M. *J. Am. Chem. Soc.* **1979**, *101*, 4433−4453.

(11) Polam, J. R.; Wright, J. L.; Christensen, K. A.; Walker, F. A.; Flint, H.; Winkler, H.; Grodzicki, M.; Trautwein, A. X. *J. Am. Chem. Soc.* **1996**, *118*, 5272−5276.

(12) Bühl, M. *Chem. Phys. Lett.* **1997**, *267*, 251−257.

(13) Godbout, N.; Malkin, V. G.; Malkina, O. L.; Salahub, D. R. *J. Chem. Phys.*, submitted for publication.

(14) Eriksson, L.; Malkina, O. L.; Malkin, V. G.; Salahub, D. R., *Int. J. Quantum Chem.* **1997**, *63*, 575−583.

(15) Fedotov, M. A.; Malkina, O. L.; Malkin, V. G. *Chem. Phys. Lett.* **1996**, *258*, 330−335.

(16) Chan, J. C. C.; Au−Yeung, S. C. F. *J. Phys. Chem., A* **1997**, *101*, 3637−3640.

(17) Godbout, N.; Oldfield, E. *J. Am. Chem. Soc.* **1997**, *119*, 8065−8069.

(18) de Dios, A. C.; Pearson, J. G.; Oldfield, E. *Science* **1993**, *260*, 1491−1496.

(19) Oldfield, E. *J. Biomol. NMR* **1995**, *5*, 217−225.

(20) Frisch, M. J.; Trucks, G. W.; Schlegel, H. B.; Gill, P. M. W.; Johnson, B. G.; Robb, M. A.; Cheeseman, J. R.; Keith, T.; Petersson, G. A.; Montgomery, J. A.; Raghavachari, K.; Al-Laham, M. A.; Zakrzewski, V. G.; Ortiz, J. V.; Foresman, J. B.; Cioslowski, J.; Stefanov, B. B.; Nanyakkara, A.; Challacombe, M.; Peng, C. Y.; Ayala, P. Y.; Chen, W.; Wong, M. W.; Andres, J. L.; Replogle, E. S.; Gomperts, R.; Martin, R. L.; Fox, D. J.; Binkley, J. S.; Defrees, D. J.; Baker, J.; Stewart, J. P.; Head-Gordon, M.; Gonzalez, C.; Pople, J. A., *GAUSSIAN 94*, Revision E.2; Gaussian, Inc.: Pittsburgh, PA, 1997.

(21) Cheeseman, J. R.; Trucks, G. W.; Keith, T. A.; Frisch M. J. *J. Chem. Phys.* **1996**, *104*, 5497−5509.

(22) Salzmann, R.; Ziegler, C. J.; Godbout, N.; McMahon, M.; Suslick, K. S.; Oldfield, E., *J. Am. Chem. Soc*., submitted for publication.

(23) Salzmann, R.; Oldfield, E., to be submitted for publication.

(24) Abola, E. E.; Bernstein, F. C.; Bryant, S. H.; Koetzle, T. F.; Weng, J. "Protein Data Bank" in Crystallographic Databases − Information Content, Software Systems, Scientific Applications; Data Commission of the International Union of Crystallography.

(25) Mink, L. M.; Polam, J. R.; Christensen, K. A.; Bruck, M. A.; Walker, F. A. *J. Am. Chem. Soc*. **1995**, *117*, 9329−9339.

(26) Naiyin, L.; Coppens, P.; Landrum, J. *Inorg. Chem.* **1988**, *27*, 482−488.

(27) Chesnut, D. B.; Moore, K. D. *J. Comput. Chem.* **1989**, *10*, 648−659.

(28) Wachters, A. J. H. *J. Chem. Phys.* **1970**, *52*, 1033−1036; Wachters, A. J. H. IBM Technology Report RJ584, 1969.

(29) Basis sets were obtained from the Extensible Computational Chemistry Environment Basis Set Database, Version 1.0, as developed and distributed by the Molecular Science Computing Facility, Environmental and Molecular Sciences Laboratory, which is part of the Pacific Northwest Laboratory, P.O. Box 999, Richland, WA 99352, U.S.A., and is funded by the U.S. Department of Energy. The Pacific Northwest Laboratory is a multiprogram laboratory operated by Battelle Memorial Institute for the U.S. Department of Energy under Contract DE-AC06−76RLO 1830. Contact David Feller, Karen Schuchardt, or Don Jones for further information.

(30) Becke, A. D. *J. Chem. Phys.* **1993**, *98*, 5648−5652.

(31) Lee, C.; Yang, W.; Parr, R. G. *Phys. Rev. B* **1988**, *37*, 785−789.

(32) Le, H.; Pearson, J. G.; de Dios, A. C.; Oldfield, E. *J. Am. Chem. Soc.* **1995**, *117*, 3800−3807.

(33) Heller, J.; Laws, D. D.; King, D. S.; Wemmer, D. W.; Pines, A.; Havlin, R. H.; Oldfield, E. *J. Am. Chem. Soc.* **1997**, *119*, 7827−7831.

(34) Baltzer, L.; Landergren, M. *J. Am. Chem. Soc.* **1990**, *112*, 2804−2805.

(35) Norvell, J. C.; Nunes, A. C.; Schoenborn, B. P. *Science* **1975**, *190*, 568−570.

(36) Powers, L.; Sessler, J. L.; Woolery, G. L.; Chance, B. *Biochemistry* **1984**, *23*, 5519−5523.

(37) Bianconi, A.; Congiu-Castellano, A.; Durham, P. J.; Hasnain, S. S.; Phillips, S. *Nature* **1985**, *318*, 685−687.

(38) Kuriyan, J.; Wilz, S.; Karplus, M.; Petsko, G. A. *J. Mol. Biol.* **1986**, *192*, 133−154.

(39) Yang, F.; Phillips, G. N., Jr. *J. Mol. Biol.* **1996**, *256*, 762−774.

(40) Lim, M.; Jackson, T. A.; Anfinrud, P. A. *Science* **1995**, *269*, 962−966.

(41) Ivanov, D.; Sage, J. T.; Keim, M.; Powell, J. R.; Asher, S. A.; Champion, P. M. *J. Am. Chem. Soc.* **1994**, *116*, 4139−4140.

(42) deDios, A. C.; Earle, E. J. *J. Phys. Chem. A* **1997**, *101*, 8132−8134.

(43) Havlin, R. H.; Godbout, N.; Salzmann, R.; Wojdelski, M.; Arnold, W. A.; Schulz, C. E.; Oldfield, E., *J. Am. Chem. Soc*., in press.

(44) Dufek, P.; Blaha, P.; Schwarz, K. *Phys. Rev. Lett.* **1995**, *75*, 3545−3548.

(45) Grodzicki, M.; Flint, H.; Winkler, H.; Walker, F. A.; Trautwein, A. X. *J. Phys. Chem.* **1997**, *101*, 4202−4207.

(46) Kobayashi, H.; Maeda, Y.; Yanagawa, Y. *Bull. Chem. Soc. Jpn.* **1970**, *43*, 2342−2346.

(47) Cooke, R.; Debrunner, P. *J. Chem. Phys.* **1968**, *48*, 4532−4537.

(48) Parak, F.; Thomanek, U. F.; Bade, D.; Wintergerst, B. *Z. Naturforsch.* **1977**, *32*, 507−512.

(49) McMahon, M.; deDios, A. C.; Godbout, N.; Salzmann, R.; Laws, D. D.; Le, H.; Havlin, R. H.; Oldfield, E., *J. Am. Chem. Soc*., submitted for publication.